══════ RESEARCH ARTICLES ══════
══════ ОРИГИНАЛЬНЫЕ СТАТЬИ ══════

ESTIMATION OF CARBON DIOXIDE FLUXES ON A RIDGE-HOLLOW BOG COMPLEX USING A HIGH RESOLUTION ORTHOPHOTOPLAN

Dmitry G. Ivanov[1,*] [iD], **Ivan P. Kotlov[1]** [iD], **Tatiana Yu. Minayeva[2]** [iD], **Julia A. Kurbatova[1]** [iD]

[1]*A.N. Severtsov Institute of Ecology and Evolution of RAS, Russia*
[2]*Institute of Forest Science of RAS, Russia*
*e-mail: ivanovdg19@gmail.com

The use of unmanned aerial vehicles for detailed mapping of ecosystems has become increasingly important in recent years. As one of the main terrestrial carbon reserves, peatland ecosystems are of the great interest in obtaining highly detailed orthophotoplans. At the same time, there is a lack of publications devoted to the total carbon dioxide fluxes in each type of bog microforms. This paper presents the results of our study, which aimed to develop methods for mapping peatland microlandscapes and for estimation of integral carbon dioxide fluxes between the peatland surface and the atmosphere. Based on a highly detailed orthophotoplan compiled using unmanned aerial vehicles, we assessed the areas of major microform groups (swamps, hollows, and ridges) in a bog located in the Central Forest State Nature Biosphere Reserve (European Russia). The classification accuracy ranged from 79% to 93%. The areas of ridges, hollows, and swamps were 0.16 km², 0.32 km², and 0.12 km², respectively. To make an integral estimation of carbon dioxide fluxes, we used earlier data on carbon dioxide emissions (ecosystem respiration), uptake (gross ecosystem exchange), and balance (net ecosystem exchange) measured by soil chamber method on representative experimental plots of respective microform types. After recalculating fluxes to areas of microforms, the integral values for different classes in the summer seasons of 2014, 2016 and 2017 were 15–91 kg $CO_2 \times h^{-1}$ for ecosystem respiration, 21–190 kg $CO_2 \times h^{-1}$ for gross ecosystem exchange, and from -122 kg $CO_2 \times h^{-1}$ to 41 kg $CO_2 \times h^{-1}$ for net ecosystem exchange. The results of the study confirmed that highly detailed orthophotoplans, obtained with the use of unmanned aerial vehicles, make it possible to distinguish the boundaries of such bog microforms as swamps, hollows and ridges with a high accuracy, despite the presence of some errors in the classification. The study of the structural and functional organisation of the bog should be carried out with considering its seasonal and interannual dynamics as well as all microform types.

Key words: chamber method, CO_2, groundwater level, microtopography, peatland, spatial heterogeneity, unmanned aerial vehicle

Introduction

Various peatland types, including the shallow peat soils, cover more than 3.46×10^6 km² of North American and the Eurasian taiga and subarctic zones and store $270–370 \times 10^{15}$ g carbon. This is about 30% of the total carbon store in soils of the world (Joosten & Clark, 2002). Peatlands are the only terrestrial ecosystem to accumulate carbon in peat deposits on a geological time scale. Also, they are complex dynamic systems both in time and space, and therefore traditionally, when studying their functional properties based on an integral landscape classification, spatial heterogeneity of all peatland components has been taken into account (Masing, 1974; Wieder & Vitt, 2006). The spatial structure of mire landscapes as well as species composition and quantitative characteristics of the vegetation cover have changed considerably, even within a few decades (Bogdanovskaya-Gienef, 1969; Johansson et al., 2006), under the influence of natural and human-induced processes. Changes in the structural peatland characteristics, such as the area and canopy density of forested tracts, surface slope, and microtopography, also lead to changes in their functional characteristics, namely rewetting or drainage, increased rates of peat accumulation or mineralisation in some parts of the peatland (Minayeva & Sirin, 2012), and, accordingly, associated biogeochemical processes (McPartland et al., 2019).

In recent years, biogeochemical processes in terrestrial ecosystems have been discussed in the context of climate regulation functions due to the pressing challenge of global climate change. In that context, wetland ecosystems act as sinks or sources of greenhouse gases, with carbon dioxide being one of the most important ones (IPCC, 2014; Zamolodchikov et al., 2017). Evidence of a

declining trend in ground water levels throughout Europe has been published (Swindles et al., 2019). Changes in the area ratio of greenhouse gas sources and sinks in the course of human transformation of natural ecosystems is the basis for national reporting on climate (IPCC, 2014), in particular for the indicators of «nationally defined contributions (NDCs)» under the Paris Agreement (Anisha et el., 2020). For this purpose, it is essential to develop a system of indicators to characterise greenhouse gas fluxes based on structural and functional characteristics of the ecosystems (Kurbatova et al., 2009). With the assessment of the structural and functional organisation of terrestrial ecosystems being an overarching priority, the scientific community needs to optimise existing research methods and create new ones based on the integration of direct experimental observations, remote sensing data, and modelling (Puzachenko et al., 2014).

Two main methods presently used to experimentally assess CO_2 fluxes between the atmosphere and the peatland surface are eddy covariance (EC) and chamber measurements. The EC method provides direct assessments of the CO_2 balance at a spatial averaging level comparable to the size of the studied ecosystem. The EC method has been widely used worldwide (Lund et al., 2010; Zeng et al., 2020), but only in isolated instances in Russia (Zamolodchikov et al., 2011; Miglovets et al., 2014; Krivenok et al., 2019). Contrastingly, the bulk of experimental data on CO_2 fluxes, including peatlands, has been obtained using the chamber method that allows measuring CO_2 fluxes at microform level (Glagolev, 2010; Mikhaylov et al., 2011; Golovatskaya & Dyukarev, 2012; Molchanov & Olchev, 2016; Volkova et al., 2017; **Bond-Lamberty & Thomson, 2018**). To assess integration fluxes for the whole peatland (or its components) using the chamber measurements, one needs to know the spatial structure of the peatland and its seasonal and annual dynamics.

The development of remote sensing methods using unmanned aerial vehicles (UAVs) provides new opportunities for environmental research in various fields. However, the use of UAVs for studying biogeochemical processes is currently still very limited (Alexander & Harvey, 2014; Lehmann et al., 2016; Arroyo-Mora et al., 2018). At the same time, remote sensing from a UAV provides information on the structural organisation of peatland that can be used to assess the functioning of the mire ecosystem as a whole.

The purpose of this study was to obtain integrated estimates of CO_2 fluxes for a bog, using data from long-term observations of CO_2 fluxes at the microtopography level and the results of remote image analyses of the bog using UAVs. This research is focused on the development of understanding of the structural and functional organisation of the southern taiga ecosystems, using modern experimental methods of environmental studies.

Material and Methods
Site description
This research was a part of the South Valdai Ecological Observatory «Okovsky Forest» (SVEO) integrated program of the A.N. Severtsov Institute of Ecology and Evolution of RAS, located in the Central Forest State Nature Biosphere Reserve (CFR) in Tver Region (European Russia). The CFR's ecosystems are objects of long-term monitoring of biogeochemical and biogeophysical processes based on integrated studies of various spatial and temporal resolutions (Kurbatova et al., 2009; Novenko et al., 2009).

The experimental studies were carried out on the bog Staroselsky Mokh (Fig. 1). The bog is located in the southeast part of the Valdai Hills within the boundaries of the CFR's buffer zone (56.47° N, 33.04° W).

Fig. 1. Location of the study area (right panel), and satellite image of the peat bog. Red line indicates borders of the ridge-hollow complex; black point in the centre shows the location of CO_2 measurements.

Nosova (2009) and Novenko (2011) dated the age of near-bottom peat deposits by means of the ^{14}C isotope analysis at some sampling spots. The age varied from 6500 to 9000 years ago (BP), which marks the beginning of the peatland formation in the boreal stage of the Holocene. Throughout this period, the microlandscapes of the mire developed from the eutrophic to mesotrophic and then oligotrophic stages. The study area was formed as a separate peatland and later merged with other tracts of the peatland. It has been in steady dynamics over the last 2000 years.

The bog Staroselsky Mokh covers an area of 6.17 km^2. The mean peat depth is 3.2 m (maximum 5.5 m). The ground water level (GWL) varies from 10 cm above to 60 cm below the surface. The vegetation cover of the peatland is typical for bogs in the southern taiga subzone. The object of this study was ridge-hollow complexes (RHC) located on the gentle slopes of the southern domed part of the bog, which are drained to varying degrees.

According to the accepted mire vegetation zoning system (Safronova & Yurkovskaya, 2015), the study area is located in the southern taiga subzone, while the peatland type (Yurkovskaya, 1992) belongs to the category of Eastern European *Sphagnum* bogs that dominate much in European Russia (Sirin et al., 2014, 2017). The most comprehensive vegetation descriptions and geobotanical mapping of the bog were made by Minayeva with colleagues (Botch & Minayeva, 1991; Minayeva et al., 2007). We divided 25 plant associations to 12 association complexes

within microlandscape borders based on over 300 geobotanical descriptions. RHC included typical sparsely forested ridges of *Ledo-Sphagnetum fusci* Du-Ruetz, 1921 and hollows with communities of *Rhynchosporion albae* Koch, 1926. At the bottom of the slopes, some hollows have large degraded patches as a result of rapid hydrology changes and freezing-thawing processes that have formed mud bottom flarks, called by some authors «rimpi» (Joosten et al., 2017). They are completely devoid of vegetation or have sparse stands dominated by *Sphagnum cuspidatum* Ehrh. ex Hoffm. and *Odontoschisma fluitans* (Nees) L.Söderstr. & Váňa.

In this study, all microform types found in the ridge-hollow complex were combined into three main classes (Fig. 2). The class «swamps» included ponds, periodically flooded flarks with a continuous *Sphagnum* cover, and degraded mud bottom flarks with virtually no vegetation. The class «hollows» contained generally accepted microform types, such as hollows with no open water and lawns. The class of «ridges» consisted of flat ridges, high ridges, and hummocks. Periodically flooded hollows were well distinguished from permanently flooded ones in the analysis of seasonal GWL dynamics, as well as visually in the landscape when comparing images from different periods. Dominant plant species of each microform type are shown in Table 1. Scientific names of vascular plants and mosses are used according to POWO (http://www.plantsoftheworldonline.org/) and Hodgetts et al. (2020), respectively.

Fig. 2. Examples of dominant bog microforms (16.08.2019). Designations: 1 – swamps, 2 – hollows, 3 – ridges.

Table 1. Dominant plant species of microform types in the study area

Microform	Herbaceous plants	Shrubs	Mosses
Ridges and hummocks	*Drosera rotundifolia* L., *Rhynchospora alba* (L.) Vahl, *Eriophorum vaginatum* L.	*Chamaedaphne calyculata* (L.) Moench, *Andromeda polifolia* L., *Rhododendron tomentosum* Harmaja, *Vaccinium oxycoccos* L.	*Sphagnum fuscum* (Schimp.) H. Klinggr., *S. medium* Limpr., *S. angustifolium* (C.E.O. Jensen ex Russow) C.E.O. Jensen
Hollows	*Scheuchzeria palustris* L., *Rhynchospora alba* (L.) Vahl, *Carex limosa* L., *Drosera anglica* Huds., *Eriophorum vaginatum* L.	–	*Sphagnum fallax* (H. Klinggr.) H. Klinggr., *S. majus* (Russow) C.E.O. Jensen, *S. cuspidatum* Ehrh. ex Hoffm., *S. balticum* (Russow) C.E.O. Jensen
Swamps	*Rhynchospora alba* (L.) Vahl	–	*S. cuspidatum* Ehrh. ex Hoffm., *Odontoschisma fluitans* (Nees) L. Söderstr. & Váňa, *Gymnocolea inflata* (Huds.) Dumort.

UAS Platform and Sensor Technique

We photographed the ridge-hollow complex on 27.07.2019 at 100 m above the surface with continuous cloud cover to ensure uniform shadowless lighting of the entire orthophotoplan. We used a Mavic 2 Pro (DJI, China) UAV equipped with the built-in L1D-20c 20-megapixel camera (Hasselblad, Sweden) mounted on a 3-axis suspension. The camera includes 1-inch sensor (13.2 × 8.8 mm), which allows one shooting frames of 5472 × 3648 pixels, and a lens with a focal length of 28 mm and a viewing angle of 77°. The exposure time was set automatically from 1/120 to 1/320 at a constant F7.1 aperture and a light sensitivity of 400 ISO. The flight plan was made in the program Drone Harmony (Switzerland) with a front and side overlap of 70% and a flight speed of 8 m/s. The UAV was equipped with a built-in GPS/GLONASS system with an average positioning accuracy of ± 0.3 m.

Data processing and classification

A total of 731 images with 2.4 cm/pixel resolution were obtained. Each image included geolocation data at the central point (latitude, longitude and altitude in WGS84 geodetic system). All images were recorded in DNG format and further processed in Adobe Lightroom 8.3 (Adobe Inc., USA), which included the bringing to standard brightness and contrast. An orthophotoplan mosaic (Fig. 3a, Fig. 4a) was composed of georeferenced images in Agisoft Photoscan Professional 1.4.5 (Agisoft LLC, Russia).

The boundaries of microform classes based on the orthophotoplan were delineated in ArcMap 10.6.1 (ESRI Inc., USA). The classification procedure consisted of the following steps:

1) Establishment of 100 supervision polygons for each of the three classes (ridges, hollows, swamps).

2) Classification using the «Maximum Likelihood Classification» tool that calculates the odds for a cell to belong to one of the classes based on the calculated mean value vector and covariance matrix (Fig. 3b).

3) Application of 50 cycles of the «Majority Filter» tool to remove small artifacts by replacing raster image cells based on the value of most adjacent cells.

4) Re-scale of each pixel by four times to facilitate raster image translation into vector. The resulting class map is very detailed, and accuracy of boundaries between classes remains high.

5) Raster vectorisation: 270 000 polygons were obtained.

6) Using the «Eliminate» tool to remove too small polygons.

7) Smoothing the polygon corners and making the microform edges as close to the natural ones as possible with Smooth polygon (Fig. 3c, Fig. 4b).

A layer with 501 check points (167 points per class), evenly distributed over the study area, was created to check the classification accuracy. The classes of points were automatically defined in one of the fields and the true classes were manually recorded in the other field. Then, the «Compute Confusion Matrix» tool was used to determine the percentage of correspondence of these two fields for each class. The confusion matrix (Table 2) shows vertically the number of points assigned to a particular class from all points in each class. For example, out of 167 points assigned by the algorithm to swamps, 138 points turned out to be real swamps, 21 hollows, and eight ridges and hummocks. Producer's accuracy (%) is the ratio between correctly classified objects and reference samples within a class. User's accuracy (%) is the ratio between correctly classified objects and the total number of samples assigned to a class.
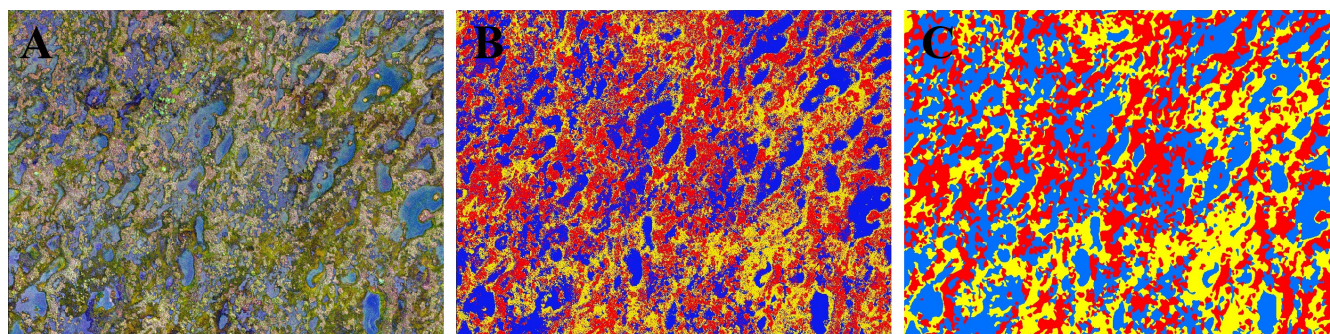
Fig. 3. An orthophotoplan section (A) compared with the final classification before (B) and after noise filtration (C), with swamps in blue, hollows are marked in yellow, and ridges in red.
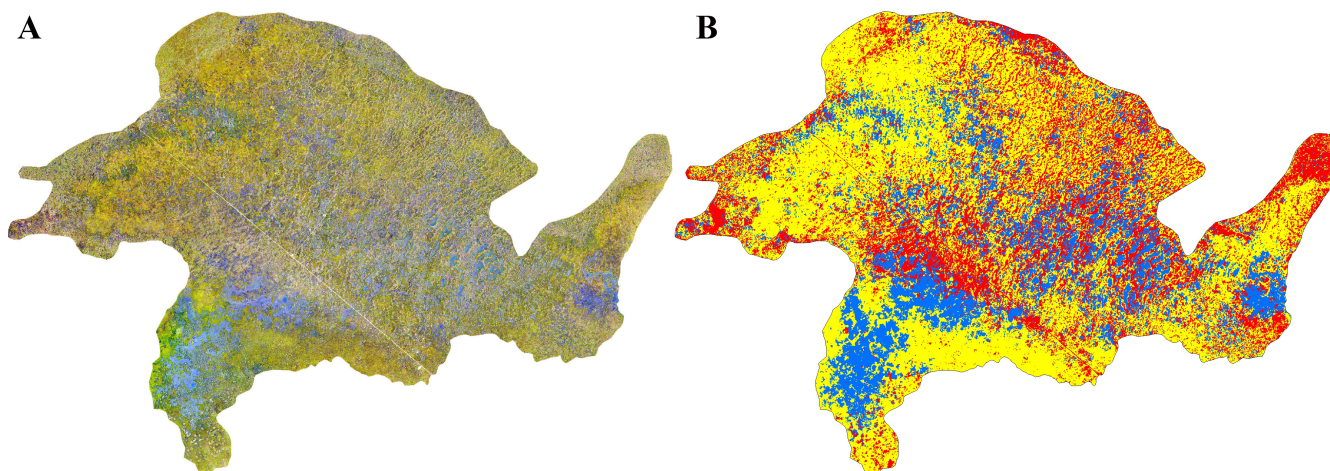

Fig. 4. Ridge-hollow complex on the orthophotoplan (A) and classified map (B). Designations: red – ridges, yellow – hollows, blue – swamps.

Table 2. Confusion matrix and accuracy results of classification and class areas

Microforms	Ridges and hummocks	Hollows	Swamps	Producer's accuracy, %	User's accuracy, %	Area, km^2	% from total area
Ridges and hummocks	145	21	8	83	87	0.16	27
Hollows	17	141	21	79	84	0.32	53
Swamps	5	5	138	93	83	0.12	20
Total	167	167	167	85	85	0.60	100

The final microform classification maps are presented in Fig. 4b. Semi-automatic object-oriented supervised classification and subsequent noise filtration showed an overall accuracy level of 85%, while the concordance coefficient of automatic and manual checking was 0.77. The microforms of flooded swamps (93%) were the most successfully distinguished, as they had higher colour contrast. The classification of ridges (83%) and hollows (79%) was less accurate, because the two classes had relatively similar colour characteristics (Table 2). Classification errors mainly occurred at smooth boundaries and transitions between microforms, and, in our opinion, had little effect on the final area estimation. According to the obtained estimates, the area of the ridge-hollow complex was 0.6 km^2, of which 0.16 km^2 (27%) were covered with hummocks and ridges, 0.32 km^2 (53%) were hollows, and 0.12 km^2 (20%) were swamps. The area under buildings and wooden plank roads was 0.01 km^2.

CO_2 flux measurements

The measurement technique is described in detail in Ivanov et al. (2017). CO_2 fluxes between the peatland surface and the atmosphere were measured using soil chambers in the central part of the ridge-hollow complex, where representative microform types, including ridges, hollows and swamps, were selected (Fig. 5A,B,C).

Observations were made during four summer seasons (June – August) in 2014–2017. Compared to mean long-term data from the weather station «Forest Reserve», located 5 km from the measurement spots, the summer periods 2014 and 2016 can be characterised as hot with moisture content close to the long-term mean, 2015 as hot and dry, 2017 and 2019 as warm with moisture content above average.
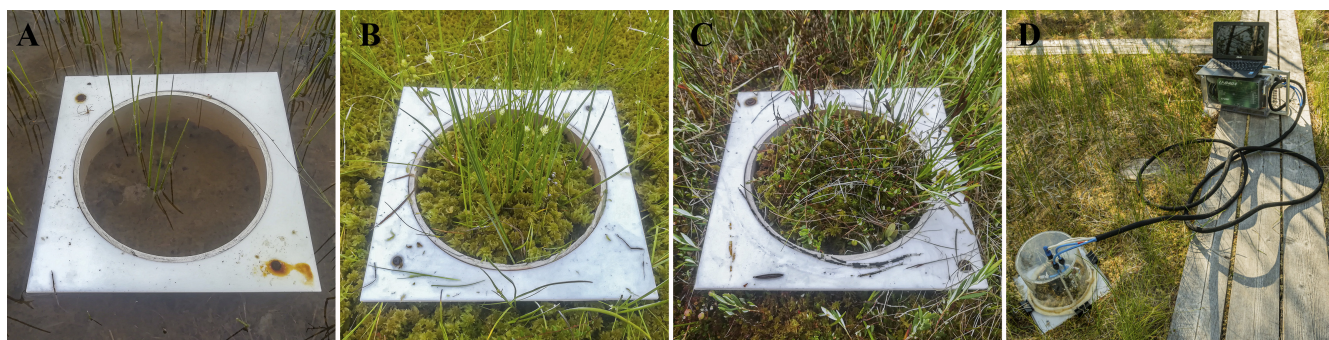
Fig. 5. Selected microforms for closed chamber flux measurements. Designations: A – *Rhynchospora* swamp, B – *Sphagnum fallax* hollow, C – *Sphagnum magellanicum* ridge, D – chamber with gas analyser.

CO_2 fluxes were measured using transparent cylindrical soil chambers made of plexiglass (Fig. 5D). The chambers were 16 cm high and 19 cm in diameter. They were mounted on cylindrical bases, cut to 15 cm into the soil. We made five repetitions on ridges, three repetitions on hollows, and two repetitions on swamps. The small number of repetitions on the swamps and hollows were due to the fact that these were considered one class during the CO_2 flux measurements and separated only later. The chamber was covered with a lightproof cover to measure CO_2 emissions (R – ecosystem respiration), and the cover was removed to measure CO_2 balance (NEE – net ecosystem exchange). Carbon dioxide uptake (GEE – gross ecosystem exchange) during photosynthesis was calculated as a difference between R and NEE (Luus & Lin, 2017). CO_2 concentration inside the chamber was measured with the frequency of 1 Hz on Li-820 infrared gas analyser (Li-Cor Inc., USA). Exposure times were 180–220 sec. The flux was calculated on the basis of exponential function in TableCurve 2D (Systat Software Inc., USA). Negative NEE values correspond to the prevalence of CO_2 absorption by ecosystem, while positive values to the prevalence of CO_2 emission to atmosphere.

Integral CO_2 fluxes were calculated as:

$$F_{ic} = F_{avc} \times S_c,$$

where, F_{ic} – integral flux (R, GEE, NEE) for the microform class (kg $CO_2 \times h^{-1}$), F_{avc} – average flux value for a class over the summer period (mg $CO_2 \times m^{-2} \times h^{-1}$), S_c – class area (km^2).

The ground water level was measured in plastic tubes 1.5 m long and 2 cm in diameter, perforated along the entire length. The tubes were constantly placed in the peat for three repetitions near each microform type. The water level was determined by a hose with a rubber bulb at the end, with which the air was pumped. The hose was immersed into the tube until bubbles appeared in the water. Then the length of the removed hose was measured.

Results

CO_2 fluxes at the ridge-hollow complex differed greatly, between years as well as between microform classes. The dynamics as well as spatial and temporal variability of the CO_2 fluxes for 2014–2015 are described in detail in Ivanov et al. (2017), where fluxes on ridges and hollows were combined under one microform type. Here is general information on CO_2 fluxes during 2014–2017 (Fig. 6).

The highest CO_2 emissions in all the summer periods were observed on the ridges, while they were 30–70% lower in the hollows and swamps which, in general, did not differ from each other. When comparing summer seasons, the years 2014–2016 with normal and insufficient moisturising had similar emission values, with mean emissions measuring 482–548 mg $CO_2 \times m^{-2} \times h^{-1}$ on ridges and 186–362 mg $CO_2 \times m^{-2} \times h^{-1}$ in swamps and hollows. The wet summer of 2017 was considerably different from the other observation years. This year CO_2 emissions were 2–3 times lower than in the previous years and measured 254 mg $CO_2 \times m^{-2} \times h^{-1}$ on ridges and 92–122 mg $CO_2 \times m^{-2} \times h^{-1}$ in swamps. The CO_2 absorption during photosynthesis in 2014–2015 was approximately the same in all microform classes (308–391 mg $CO_2 \times m^{-2} \times h^{-1}$). In 2016, the absorption of CO_2 during photosynthesis was the greatest for all microforms and varied from 439 mg $CO_2 \times m^{-2} \times h^{-1}$ in the swamps to 680 mg $CO_2 \times m^{-2} \times h^{-1}$ on the ridges. In 2017, the lowest average GEE values for all years were

observed in the swamps and hollows (202 mg $CO_2 \times m^{-2} \times h^{-1}$ and 311 mg $CO_2 \times m^{-2} \times h^{-1}$, respectively), while the absorption on the ridges was close to the values of 2016, i.e. 659 mg $CO_2 \times m^{-2} \times h^{-1}$. In 2014–2015, the CO_2 balance in swamps and hollows was close to zero (from -72 mg $CO_2 \times m^{-2} \times h^{-1}$ to 28 mg $CO_2 \times m^{-2} \times h^{-1}$), and above zero on ridges (167–312 mg $CO_2 \times m^{-2} \times h^{-1}$). In other years, the balance for all microforms was negative, i.e. CO_2 deposition prevailed over emission, with the maximum negative values noted in hollows and swamps in 2016, and on ridges in 2017. Based on the presented results, the ridge-hollow complex can be characterised as a CO_2 sink.

According to the data from hydrological observations carried out under the CFR's long-term stationary observation programs, the water level in hollows in the central part of the RHC varied during the summers of 2014–2019 from 5–10 cm above to 20–30 cm below the surface (Fig. 7). The lowest level was noted in the dry year 2015, when the water in the hollows dropped to 4–20 cm below the surface, and in the second half of 2014 when GWL dropped to 18 cm below the surface. In 2016 and 2019, the water level was similar and measured 2–10 cm below the surface. In 2017, due to abundant precipitation, the GWL throughout most of the summer was above the surface (from -0.5 cm to 4.0 cm). Large differences in the depth of ground waters lead to a considerable disparity in the ratio of areas of ridges, hollows and swamps during the summer. In addition, variation in water level in the peat undoubtedly affects the depth of aerated peat layer as the main source of CO_2, as well as the activity of CO_2 uptake by plants. Therefore, to estimate the CO_2 fluxes per unit area, we took a narrow range of ground water levels in hollows in the central part of the CFR measured on the day of orthophotoplan survey (± 1 day), which varied from 0 cm to 2 cm below the surface. The corresponding dates of CO_2 flux measurements in previous years were selected for this range: 21.06.2014, 25.06.2014, 03.07.2014, 21.06.2016, 22.07.2016, 28.07.2016, 05.08.2016, 24.08 2016, 04.06.2017, 21.06.2017, and 15.08 2017.

The selected days with this range of ground water levels differed considerably in soil and air temperatures. In 2014, it was quite cool and, at the GWL from -1 cm to 1 cm, the soil temperature was 14.6 ± 0.5°C, and the air temperature was 18.4 ± 1.8°C. In 2016, there were the warmest days with a soil temperature of 19.1 ± 1.1°C and an air temperature of 26.2 ± 3.3°C. In 2017, the days differed considerably in temperature conditions. The spread of soil temperatures was 11°C and air temperatures 13°C, with mean values close to those registered in 2014 (14.8 ± 4.0°C and 16.6 ± 4.4°C, respectively). These temperature variations resulted in a considerable difference in CO_2 fluxes for individual dates as well as between the years. Fig. 8 shows mean relative values of carbon dioxide fluxes (mg $CO_2 \times m^{-2} \times h^{-1}$) for all the selected dates. Due to differing temperature conditions, standard deviations fluctuate between 50% and 300%, especially for the CO_2 balance. However, generally, the highest emission and uptake values were observed on the ridges, and the lowest in the swamps. A negative CO_2 balance (i.e. the predominance of absorption over emission) was observed mostly in the hollows.
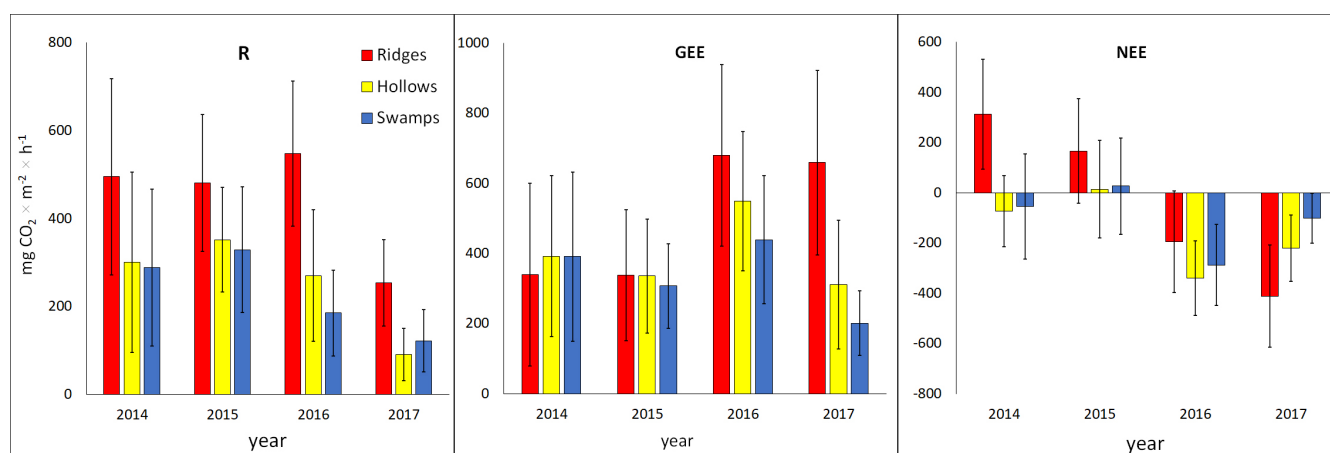

Fig. 6. Average (± SD) CO_2 emission (R), uptake (GEE) and balance (NEE) in microforms during 2014–2017 summer seasons in the study area.
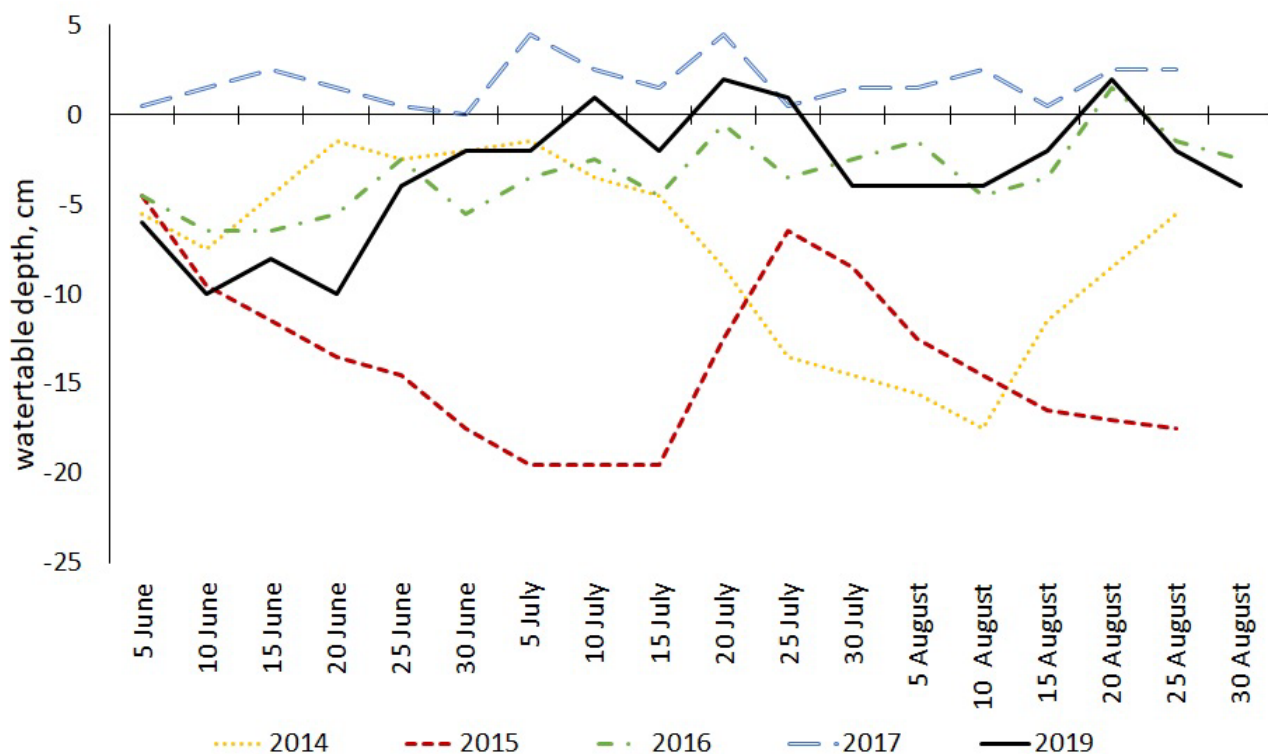
Fig. 7. Ground water level dynamics in summer seasons 2014–2019 in the study area.
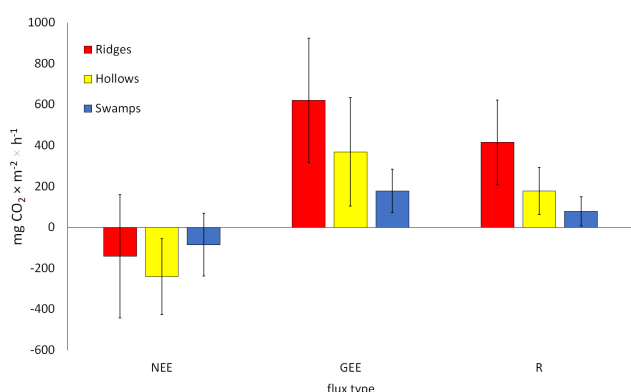

Fig. 8. Average (± SD) CO_2 emission (R), uptake (GEE) and balance (NEE) for 2014, 2016 and 2017 summer seasons in the study area.

Having re-calculated relative values of fluxes separately for each year and microform area (in km²), the ratio of CO_2 emission, uptake, and balance on ridges, in hollows and in swamps changed (Fig. 9). Differences in emissions between summer seasons corresponded to those in air and soil temperatures. In the relatively cold years of 2014 and 2017, on average 15 kg $CO_2 \times h^{-1}$ were released in the swamps, 25–39 kg $CO_2 \times h^{-1}$ in the hollows, and 38–51 kg $CO_2 \times h^{-1}$ on the ridges. At the same time in 2016, the emissions amounted to 91 kg $CO_2 \times h^{-1}$ on the ridges, 78 kg $CO_2 \times h^{-1}$ in the hollows, and virtually did not change in the swamps. In 2014, GEE in all microform classes were lower than in other years, ranging from 22 kg $CO_2 \times h^{-1}$ in the swamps to 58 kg $CO_2 \times h^{-1}$ on the ridges. In 2016, the uptake in the hollows was 40% higher than on the ridges (190 kg $CO_2 \times h^{-1}$), despite the fact that the relative GEE values on the ridges were higher. The highest GEE values compared with the other years were also observed in the swamps (52 kg $CO_2 \times h^{-1}$). In 2017, with pronounced temperature fluctuations, the uptake was at an average level compared to other years and varied from 21 kg $CO_2 \times h^{-1}$ in the swamps to 90 kg $CO_2 \times h^{-1}$ on the ridges. A positive CO_2 balance was only observed on the ridges in 2014 (41 kg $CO_2 \times h^{-1}$). Moreover, NEE values in the hollows and swamps (-35 kg $CO_2 \times h^{-1}$ and -8 kg $CO_2 \times h^{-1}$, respectively) were at the lowest negative range the same year. The highest negative balance was registered in the hollows in 2016 (-122 kg $CO_2 \times h^{-1}$) and on the ridges in 2017 (-52 kg $CO_2 \times h^{-1}$).

Integral CO_2 fluxes from the entire ridge-hollow complex also varied considerably between years. The highest CO_2 fluxes in absolute values were recorded in 2016 (R: 189 kg $CO_2 \times h^{-1}$, GEE: 355 kg $CO_2 \times h^{-1}$, NEE: 188 kg $CO_2 \times h^{-1}$). In turn, the lowest values in absolute values for NEE (-2 kg $CO_2 \times h^{-1}$) and GEE (132 kg $CO_2 \times h^{-1}$) were obtained in 2014, and for R (78 kg $CO_2 \times h^{-1}$) in 2017.
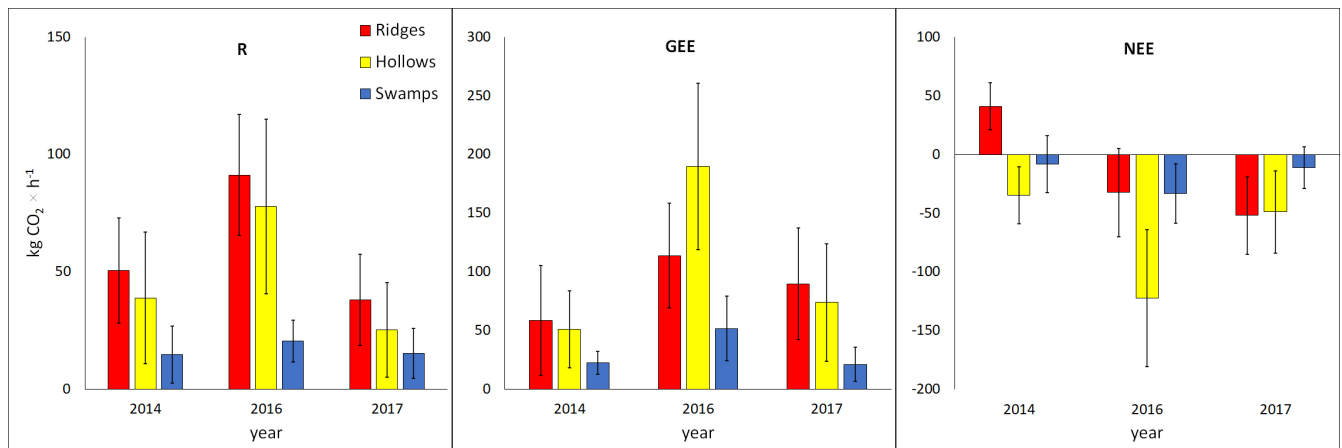
Fig. 9. Average (± SD) CO_2 emission (R), uptake (GEE) and balance (NEE) for summer seasons of 2014, 2016 and 2017 recalculated to area (km^2) for each microform type.

Discussion

Studies of CO_2 fluxes in bogs in European Russia are rather scarce in comparison with those in Asian Russia, Central and Western Europe, Canada and Alaska (Glagolev, 2010). Many studies estimated the spread of soil emission values during the growing season in the range of 60–950 mg $CO_2 \times m^{-2} \times h^{-1}$ (Smagin et al., 2000; Kurets et al., 2007; Glukhova et al., 2013; Molchanov, 2015), depending on microform types, weather conditions, as well as measurement and calculation methods. Average CO_2 balance values are from -460 mg $CO_2 \times m^{-2} \times h^{-1}$ to 970 mg $CO_2 \times m^{-2} \times h^{-1}$ (Miglovets et al., 2014). In general, the data we obtained are consistent with other studies despite they show slightly higher values in CO_2 emissions than in most studies.

Many studies also confirm the spatial heterogeneity of CO_2 fluxes following the spatial variation of environmental factors, primarily the wetland level. According to various studies (Danevčič et al., 2010; Rahman et al., 2017), there is a well-defined seasonal and long-term dynamics of the ground water level in the peatlands, which is also confirmed by our data (Fig. 7). In our study similarly to a number of other studies (Minayeva et al., 2003; Tatarinov et al., 2003; Kurbatova et al., 2004; Strack et al., 2006; Golovatskaya & Dyukarev, 2012; Urbanová et al., 2012; Molchanov, 2015; Dyukarev et al., 2019), a connection between CO_2 flux values and the ground water level, temperature of surface peat layers and the species composition of plants was noted, and a considerable difference between these parameters at the level of microforms was shown (Fig. 6, Fig. 9). This indicates the importance of microform mapping and their area estimation. A more detailed discussion of these dependencies was presented in Ivanov et al. (2017).

Previously, multispectral satellite images with resolution from 2 m to 30 m were actively used for mire classification (Adam et al., 2010; Sirin et al., 2014; Terentieva et al., 2016). At the moment, only satellite images with a resolution of 10–30 m are freely available. However, it does not allow us to take into account the areas of individual microforms, which are usually less than this resolution. This leads to an underestimation of the per unit area assessments of the mire's structural components and allows working only at the level of facies or microlandscapes (e.g. a ridge-hollow complex) or expansive homogeneous microforms (e.g. a forested bog).

Due to the high spatial variability of CO_2 fluxes, evaluating the contribution of individual microforms to the total CO_2 flux, requires not only long-term flux measurements, but also analysis of the mire structure. Thus, the quality of any study comparing different scales (e.g. individual microforms vs. association complexes) depends on the basemap quality. We used the maximum likelihood method to classify microforms based on a high resolution orthophotoplan obtained by means of a UAV equipped with an RGB camera. This resulted in an overall high accuracy, especially for swamps. The accuracy of our estimates (79–93%) is comparable to Becker (2008) who was one of the first applying highly detailed imaging of oligotrophic low-sedge pine fen in Finland using an airship and digital camera for classification of mire microforms. He also applied a maximum likelihood classification in ArcGIS with the final accuracy of 84%. Knoth et al. (2013) achieved an accuracy of 91% on a restored bog in Germany using a UAV equipped with a NIR camera, and the same classification method. Lovitt et al. (2018) used the pixel-based density slicing approach to classify hummocks, hollows and trees obtaining an average accuracy of 84%.

Peatlands are characterised by a wide variety of microforms (Mercer & Westbrook, 2016; Korpela et al., 2020), which indicates the need to analyse their

spatial structure when assessing greenhouse gas fluxes by various methods. The ground water level largely determines the ratio of microform areas (Strack et al., 2006; Rahman et al., 2017; Graham et al., 2020). Therefore, when analysing the microtopography of the swamp, it is necessary to take into account the seasonal dynamics of precipitation and the hydrological conditions of the swamp.

Conclusions

The CO_2 exchange between bog ecosystems and the atmosphere is determined by a set of factors, both abiotic and biotic. Seasonal and inter-annual variability of temperature and humidity leads to changes in the water content of bogs, and as a consequence, to changes in the CO_2 balance between the bog surface and the atmosphere. This study has confirmed that highly detailed orthophotoplans obtained by means of UAVs can be used to identify the boundaries of bog microforms, such as swamps, hollows and ridges, with rather a high accuracy, despite the presence of some classification errors. The information on the microform areas in combination with the data from experimental observations of CO_2 fluxes on representative experimental plots lets us approach the assessment of integral CO_2 fluxes for the bog as a whole. The integral flux assessment should be carried out with provision for temporal dynamics of the structural and functional organisation of the bog, which requires simultaneous observations of seasonal and inter-annual variability in the ratio between the bog microforms and CO_2 fluxes.

The CO_2 fluxes we obtained and calculated for the unit of microform area are mere estimations. Measurements of CO_2 fluxes and orthophotoplan imaging performed in various years under diverse hydrothermal conditions, as well as combining individual microform types differing in terms of water regime, vegetation composition, and position in nano-relief (ponds, swamps, mud bottom flarks, flooded hollows, lawns, ridges, hummocks) into three classes, do not let us fully estimate the total fluxes per unit area for each summer period. Some inaccurate boundaries and microforms assigned to a wrong class still pop up here and there during classification. To further improve accuracy and minimise errors, a high-resolution digital surface model should be integrated into the classification process, which can also be obtained using this UAV model. Application of tools to remove noise and artifacts not exceeding 0.5 m^2 and smooth microform borders also has its disadvantages, because, in addition to noise, some real small-size microforms, primarily ridges and swamps, can be assigned to a wrong

class, which would lead to underestimation of their contributions to the total CO_2 flux. In order to further assess contributions of peatland ecosystems and microforms to the total carbon flux, we plan to expand the research of CO_2 fluxes to other parts of the bog Staroselsky Mokh, elaborate microform types, identify their boundaries and dynamics during several seasons, keeping in mind the changes of vegetation and ground water levels using a highly detailed orthophotoplan and digital surface model.

References

Adam E., Mutanga O., Rugege D. 2010. Multispectral and hyperspectral remote sensing for identification and mapping of wetland vegetation: a review. *Wetlands Ecology and Management* 18(3): 281–296. DOI: 10.1007/s11273-009-9169-z

Alexander K.B.K., Harvey M. 2014. Cost-effective aerial imagery and soil CO_2 flux surveys for geothermal exploration. In: *Proceedings of 5th African Rift Geothermal Conference.* Vol. 2. Arusha. P. 29–31.

Anisha N.F., Mauroner A., Lovett G., Neher A., Servos M., Minayeva T., Schutten H., Minelli L. 2020. *Locking Carbon in Wetlands: Enhancing Climate Action by Including Wetlands in NDCs.* Corvallis, Oregon and Wageningen: Alliance for Global Water Adaptation and Wetlands International. 29 p.

Arroyo-Mora J.P., Kalacska M., Soffer R.J., Moore T.R., Roulet N.T., Juutinen S., Ifimov G., Leblanc G., Inamdar D. 2018. Airborne hyperspectral evaluation of maximum gross photosynthesis, gravimetric water content, and CO_2 uptake efficiency of the Mer Bleue Ombrotrophic Peatland. *Remote Sensing* 10(4): 565. DOI: 10.3390/rs10040565

Becker T., Kutzbach L., Forbrich I., Schneider J., Jager D., Thees B., Wilmking M. 2008. Do we miss the hot spots? – The use of very high resolution aerial photographs to quantify carbon fluxes in peatlands. *Biogeosciences* 5(5): 1387–1393. DOI: 10.5194/bg-5-1387-2008

Bogdanovskaya-Gienef I.D. 1969. *Patterns of the Sphagnum bogs formation (Polistovo-Lowatsky complex).* Leningrad: Nauka. 186 p. [In Russian]

Bond-Lamberty B.P., Thomson A.M. 2018. *A Global Database of Soil Respiration Data, Version 4.0.* ORNL DAAC. Availabel from https://daac.ornl.gov/cgi-bin/dsviewer.pl?ds_id=1578

Botch M.S., Minayeva T.Yu. 1991. Mires of Central Forest State Nature Reserve. In: *Mires of Protected Areas: problems of protection and monitoring.* Leningrad. P. 22–26. [In Russian]

Danevčič T., Mandic-Mulec I., Stres B., Stopar D., Hacin J. 2010. Emissions of CO_2, CH_4 and N_2O from Southern European peatlands. *Soil Biology and Biochemistry* 42(9): 1437–1446. DOI: 10.1016/j.soilbio.2010.05.004

Dyukarev E.A., Godovnikov E., Karpov D., Kurakov S., Lapshina E.D., Filippov I., Filippova N., Zarov E. 2019. Net ecosystem exchange, gross primary production and ecosystem respiration in ridge-hollow complex at Mukhrino Bog. *Geography, Environment, Sustainability* 12(2): 227–244. DOI: 10.24057/2071-9388-2018-77

Glagolev M.V. 2010. Annotated reference list of CH_4 and CO_2 flux measurements from Russian mires. *Environmental Dynamics and Global Climate Change* 1(2): 1–53. [In Russian]

Glukhova T.V., Vompersky S.E., Kovalev A.G. 2013. Emission of CO_2 from the surface of oligotrophic bogs with due account for their microrelief in the southern taiga of European Russia. *Eurasian Soil Science* 46(12): 1172–1181. DOI: 10.1134/S1064229314010050

Golovatskaya E.A., Dyukarev E.A. 2012. The influence of environmental factors on the CO_2 emission from the surface of oligotrophic peat soils in West Siberia. *Eurasian Soil Science* 45(6): 588–597. DOI: 10.1134/S106422931206004X

Graham J.D., Glenn N.F., Spaete L.P., Hanson P.J. 2020. Characterizing peatland microtopography using gradient and microform-based approaches. *Ecosystems* 23(7): 1464–1480. DOI: 10.1007/s10021-020-00481-z

Hodgetts N.G., Söderström L., Blockeel T.L., Caspari S., Ignatov M.S., Konstantinova N.A., Lockhart N., Papp B., Schröck C., Sim-Sim M., Bell D., Bell N.E., Blom H.H., Bruggeman-Nannenga M.A., Brugués M., Enroth J., Flatberg K.I., Garilleti R., Hedenäs L., Holyoak D.T., Hugonnot V., Kariyawasam I., Köckinger H., Kučera J., Lara F., Porley R.D. 2020. An annotated checklist of bryophytes of Europe, Macaronesia and Cyprus. *Journal of Bryology* 42(1): 1–116. DOI: 10.1080/03736687.2019.1694329

IPCC. 2014. *2013 Supplement to the 2006 IPCC Guidelines for National Greenhouse Gas Inventories: Wetlands.* Switzerland: IPCC. 354 p.

Ivanov D.G., Avilov V.K., Kurbatova Y.A. 2017. CO_2 fluxes at south taiga bog in the European part of Russia in summer. *Contemporary Problems of Ecology* 10(2): 97–104. DOI: 10.1134/S1995425517020056

Johansson T., Malmer N., Crill P.M., Friborg T., Aakerman J.H., Mastepanov M., Christensen T. R. 2006. Decadal vegetation changes in a northern peatland, greenhouse gas fluxes and net radiative forcing. *Global Change Biology* 12(12): 2352–2369. DOI: 10.1111/j.1365-2486.2006.01267.x

Joosten H., Clarke D. 2002. *Wise use of mires and peatlands.* Saarijärvi: International Peat Society. 303 p.

Joosten H., Moen A., Couwenberg J., Tanneberger F. 2017. Mire diversity in Europe: mire and peatland types. In: H. Joosten, F. Tanneberger, A. Moen (Eds.): *Mires and peatlands of Europe: Status, distribution and conservation.* Stuttgart: Schweizerbart Science Publishers. P. 5–64.

Knoth C., Klein B., Prinz T., Kleinebecker T. 2013. Unmanned aerial vehicles as innovative remote sensing platforms for high-resolution infrared imagery to support restoration monitoring in cut-over bogs. *Applied Vegetation Science* 16(3): 509–517. DOI: 10.1111/avsc.12024

Korpela I., Haapanen R., Korrensalo A., Tuittila E.S., Vesala T. 2020. Fine-resolution mapping of microforms of a boreal bog using aerial images and waveform-recording LiDAR. *Mires and Peat* 26: 3. DOI: 10.19189/MaP.2018.OMB.388

Krivenok L.A., Suvorov G.G., Avilov V.K., Sirin A.A. 2019. Eddy covariance measurement of CO_2, CH_4, and H_2O fluxes: Use of a mobile tower and taking into account the changing fetch. *Atmospheric and Oceanic Optics* 32(11): 942–950. DOI: 10.15372/AOO20191111 [In Russian]

Kurbatova J.A., Li C., Tatarinov F.A., Varlagin A.V., Shalukhina N.V., Olchev A.V. 2009. Modeling of the carbon dioxide fluxes in European Russia peat bogs. *Environmental Research Letters* 4(4): 045022. DOI: 10.1088/1748-9326/4/4/045022

Kurbatova J.A., Minayeva T.Yu., Tatarinov F.A., Molchanov A.G., Rusanovitch N.R. 2004. Temporal and spatial diversity of CO_2 exchange of a bog in South European Taiga. In: N.P. Laverov (Ed.): *Emissions and sinks of greenhouse gases on territory of North Eurasia.* Puschino: ONTI PNC RAS. P. 41–46. [In Russian]

Kurets V.K., Ikkonen E.N., Talanov A.V. 2007. Effects of forest reclamation on CO_2 emissions from peat and sphagno-herbal cover in a meso-oligotrophic bog. *Lesnoye Khozyaystvo* 4: 27–27. [In Russian]

Lehmann J.R., Münchberger W., Knoth C., Blodau C., Nieberding F., Prinz T., Pancotto V.A., Kleinebecker T. 2016. High-resolution classification of South Patagonian Peat Bog microforms reveals potential gaps in upscaled CH_4 fluxes by use of Unmanned Aerial System (UAS) and CIR Imagery. *Remote Sensing* 8(3): 173. DOI: 10.3390/rs8030173

Lovitt J., Rahman M.M., Saraswati S., McDermid G.J., Strack M., Xu B. 2018. UAV Remote Sensing Can Reveal the Effects of Low-Impact Seismic Lines on Surface Morphology, Hydrology, and Methane (CH_4) Release in a Boreal Treed Bog. *Journal of Geophysical Research: Biogeosciences* 123(3): 1117–1129. DOI: 10.1016/S0304-3800(03)00067-X

Lund M., Lafleur P.M., Roulet N.T., Lindroth A., Christensen T.R., Aurela M., Chojnicki B.H., Flanagank L.B., Humphreys E.R., Laurila T., Oechel W.C., Olejnik J., Rinne J., Schubert P., Nilsson M.B. 2010. Variability in exchange of CO_2 across 12 northern peatland and tundra sites. *Global Change Biology* 16(9): 2436–2448. DOI: 10.1111/j.1365-2486.2009.02104.x

Luus K.A., Lin J.C. 2017. *CARVE Modeled gross ecosystem CO_2 exchange and respiration, Alaska, 2012–2014.* Oak Ridge: ORNL DAAC. DOI: 10.3334/ORNLDAAC/1314

Masing V.V. 1974. Actual problems of classification and terminology in bog science. In: T.G. Abramova, M.S.

Boch, E.A. Galkina (Eds.): *Types of bogs in the USSR and the principles of their classification.* Leningrad: Nauka. P. 6–12. [In Russian]

McPartland M.Y., Kane E.S., Falkowski M.J., Kolka R., Turetsky M.R., Palik B., Montgomery R.A. 2019. The response of boreal peatland community composition and NDVI to hydrologic change, warming, and elevated carbon dioxide. *Global Change Biology* 25(1): 93–107. DOI: 10.1111/gcb.14465

Mercer J.J., Westbrook C.J. 2016. Ultrahigh-resolution mapping of peatland microform using ground-based structure from motion with multiview stereo. *Journal of Geophysical Research: Biogeosciences* 121(11): 2901–2916. DOI: 10.1002/2016JG003478

Miglovets M.N., Mikhaylov O.A., Zagirova S.V. 2013. Vertical CH_4 and CO_2 fluxes in plant communities of mesooligotrophic peatland of middle taiga. *Proceedings of Samara Scientific Centre RAS* 16(1): 193–197. [In Russian]

Mikhaylov O.A., Zagirova S.V., Miglovec M.N., Schneider J., Gažovič M., Kutzbach L. 2011. Evaluation of fluxes of carbon dioxide in vegetative communities of the meso-oligotrophic bog in the middle taiga. *Theoretical and Applied Ecology* 2: 44–51. [In Russian]

Minayeva T.Yu., Kurbatova J.A., Tatarinov F.A., Rusanovitch N.R. 2003. Seasonal dynamics of vegetation as a factor in CO_2 gas exchange formation between surface and atmosphere in a bog. In: N.P. Laverov (Ed.): *Emissions and sinks of greenhouse gases on territory of North Eurasia.* Puschino: ONTI PNC RAS. P. 80–81. [In Russian]

Minayeva T.Yu., Glushkov I.V., Nosova M.B., Starodubtseva O.A., Kurayeva E.N., Volkova E.M. 2007. Essay on the bogs of the Central Forest State Nature Reserve. *Proceedings of the Central Forest State Nature Reserve* 4: 267–296. [In Russian]

Minayeva T.Yu., Sirin A.A. 2012. Peatland Biodiversity and Climate Change. *Biology Bulletin Reviews* 2(2): 164–175. DOI: 10.1134/S207908641202003X

Molchanov A.G. 2015. Gas exchange in sphagnum mosses at different near-surface groundwater levels. *Russian Journal of Ecology* 46(3): 230–235. DOI: 10.1134/S1067413615030066

Molchanov A.G., Olchev A.V. 2016. Model of CO_2 exchange in a sphagnum peat bog. *Computer Research and Modeling* 8(2): 369–377. DOI: 10.20537/2076-7633-2016-8-2-369-377 [In Russian]

Novenko E.Y., Volkova E.M., Nosova N.B., Zuganova I.S. 2009. Late Glacial and Holocene landscape dynamics in the southern taiga zone of East European Plain according to pollen and macrofossil records from the Central Forest State Reserve (Valdai Hills, Russia). *Quaternary International* 207(1–2): 93–103. DOI: 10.1016/j.quaint.2008.12.006

Novenko. E.Y. 2011. *Dynamics of forest ecosystems of the South of Valdai Upland in Late Pleistocene and Holocene.* Moscow: GEOS. 112 p. [In Russian]

Nosova M.B. 2009. Holocene spore-pollen diagrams as information source about prehistoric antropogenic activity (a case study from Central Forest natural reserve).

Bulletin of Moscow Society of Naturalists 114(3): 30–36. [In Russian]

Puzachenko Y.G., Sandlersky R.B., Krenke A.N., Puzachenko Y.M. 2014. Multispectral remote information in forest research. *Contemporary Problems of Ecology* 7(7): 838–854. DOI: 10.1134/S1995425514070087

Rahman M.M., McDermid G.J., Strack M., Lovitt J. 2017. A new method to map groundwater table in peatlands using unmanned aerial vehicles. *Remote Sensing* 9(10): 1057. DOI: 10.3390/rs9101057

Safronova I.N., Yurkovskaya T.K. 2015. Zonal regularities of vegetation cover on plains of the European Russia and their cartographic representation. *Botanicheskii Zhurnal* 100(11): 1121–1141. [In Russian]

Sirin A.A., Maslov A.A., Valyaeva N.A., Tsyganova O.P., Glukhova T.V. 2014. Mapping of peatlands in the Moscow oblast based on high-resolution remote sensing data. *Contemporary Problems of Ecology* 7(7): 808–814. DOI: 10.1134/S1995425514070117

Sirin A., Minayeva T., Yurkovskaya T., Kuznetsov O., Smagin V., Fedotov Yu. 2017. Russian Federation (European Part). In: H. Joosten, F. Tanneberger, A. Moen (Eds.): *Mires and peatlands of Europe: Status, distribution and conservation.* Stuttgart: Schweizerbart Science Publishers. P. 590–617.

Smagin A.V., Smagina M.V., Vomperskii S.E., Glukhova T.V. 2000. Generation and emission of greenhouse gases in bogs. *Eurasian Soil Science* 33(9): 959–966.

Strack M., Waddington J.M., Rochefort L., Tuittila E.S. 2006. Response of vegetation and net ecosystem carbon dioxide exchange at different peatland microforms following water table drawdown. *Journal of Geophysical Research: Biogeosciences* 111(G2): G02006. DOI: 10.1029/2005JG000145

Swindles G.T., Morris P.J., Mullan D.J., Payne R.J. 2019. Widespread drying of European peatlands in recent centuries. *Nature Geoscience* 12(11): 922–928. DOI: 10.1038/s41561-019-0462-z

Tatarinov F., Kurbatova J., Molchanov A., Minaeva T., Orlov T. 2003. Measuring of components of peat and ground vegetation CO_2 balance in a southern taiga peat bog. In: A. Järvet, E. Lode (Eds.): *Ecohydrological processes in Northern Wetlands. Selected papers.* Tartu. P. 215–220.

Terentieva I.E., Glagolev M.V., Lapshina E.D., Sabrekov A.F., Maksyutov S. 2016. Mapping of West Siberian taiga wetland complexes using Landsat imagery: implications for methane emissions. *Biogeosciences* 13(16): 4615–4626. DOI: 10.5194/bg-13-4615-2016

Urbanová Z., Picek T., Hájek T., Bufková I., Tuittila E.S. 2012. Vegetation and carbon gas dynamics under a changed hydrological regime in central European peatlands. *Plant Ecology and Diversity* 5(1): 89–103. DOI: 10.1080/17550874.2012.688069

Volkova E.M., Novenko E.Yu., Olchev A.V. 2017. Evaluation of the net CO_2 exchange of forest sphagnum bog based on the results of experimental observations and model calculations. In: *Carbon Balance of Western Siberian Mires in the Context of Climate Change. Proceedings of the International Conference.* Khanty-Mansiysk. P. 48–50. [In Russian]

Wieder R.K., Vitt D.H. 2006. *Boreal peatland ecosystems*. Heidelberg: Springer Science & Business Media. 448 p.

Yurkovskaya T.K. 1992. *Geography and cartography of mire vegetation in European Russia and adjacent areas*. Saint Petersburg: Komarov Botanical Institute. 265 p. [In Russian]

Zamolodchikov D.G., Karelin D.V., Karelin A.I., Oechel W.C., Hastings S.J. 2011. CO_2 flux measurements in Russian Far East tundra using eddy covariance and closed chamber techniques. *Tellus, Series B: Chemical and Physical Meteorology* 55(4): 879–892. DOI: 10.3402/tellusb.v55i4.16384

Zamolodchikov D.G., Karelin D.V., Gitarsky G.L., Blinov V.G. 2017. *Monitoring of greenhouse gases in natural ecosystems*. Saratov: Amirit. 279 p. [In Russian]

Zeng J., Matsunaga T., Tan Z.H., Saigusa N., Shirai T., Tang Y., Peng S., Fukuda Y. 2020. Global terrestrial carbon fluxes of 1999–2019 estimated by upscaling eddy covariance data with a random forest. *Scientific Data* 7(1): 313. DOI: 10.1038/s41597-020-00653-5

ОЦЕНКИ ПОТОКОВ ДИОКСИДА УГЛЕРОДА НА ГРЯДОВО-МОЧАЖИННОМ КОМПЛЕКСЕ С ИСПОЛЬЗОВАНИЕМ ВЫСОКОДЕТАЛЬНОГО ОРТОФОТОПЛАНА

Д. Г. Иванов[1,*] , И. П. Котлов[1] , Т. Ю. Минаева[2] , Ю. А. Курбатова[1]

[1]*Институт проблем экологии и эволюции имени А.Н. Северцова РАН, Россия*
[2]*Институт лесоведения РАН, Россия*
*e-mail: ivanovdg19@gmail.com

Использование беспилотных летательных аппаратов (БПЛА) для детального картографирования экосистем становится все более актуальным в последние годы. Большой интерес в получении высокодетальных ортофотопланов представляют болотные экосистемы как одни из основных наземных резервуаров углерода. При этом довольно мало работ отражает суммарные потоки CO_2 с площади каждого типа болотных микроформ. В нашей работе представлены результаты исследования, направленного на развитие методов картографирования болотных микроландшафтов и оценки интегральных потоков CO_2 между поверхностью болота и атмосферой. На основе высокодетального ортофотоплана, полученного с использованием БПЛА была выполнена оценка площади основных групп микроформ (топи, мочажины, гряды) верхового болота, расположенного на территории Центрально-Лесного государственного природного биосферного заповедника (Европейская часть России). Точность классификации составила от 79% до 93%. Площадь гряд, мочажин и топей составили 0.16 км², 0.32 км² и 0.12 км², соответственно. Для интегральной оценки потоков CO_2 были использованы проведенные ранее измерения эмиссии (R), депонирования (GEE) и баланса (NEE) CO_2 методом почвенных камер на репрезентативных экспериментальных площадках, соответствующих типам микроформ. После пересчета потоков на площади микроформ, интегральные значения для различных классов за летние сезоны 2014, 2016 и 2017 гг. составили 15–91 кг CO_2 × ч⁻¹ для R, 21–190 кг CO_2 × ч⁻¹ для GEE и от -122 кг CO_2 × ч⁻¹ до 41 кг CO_2 × ч⁻¹ для NEE. Результаты проведенного исследования подтвердили, что использование высокодетальных ортофотопланов, полученных с помощью БПЛА позволяет с довольно высокой точностью выделить границы таких микроформ верхового болота как топи, мочажины и гряды, несмотря на наличие некоторых ошибок в классификации. Обнаружено, что в отдельных случаях микроландшафты с низкими относительными значениями потоков, но большой площадью охвата являются доминантами при интегральных оценках. Показано, что исследование структурно-функциональной организации верхового болота необходимо проводить с учетом ее сезонной и межгодовой динамики с четким разделением типов микроформ.

Ключевые слова: CO_2, беспилотный летательный аппарат, метод камер, микротопография, пространственная неоднородность, торфяник, уровень грунтовых вод